




Backaction effects in cavity-coupled quantum conductorsValeriu Moldoveanu ^{1,2,*}, Ion Viorel Dinu ^{1,2}, Andrei Manolescu ³ and Vidar Gudmundsson⁴¹National Institute of Materials Physics, Atomistilor 405A, Magurele 077125, Romania²Centre International de Formation et de Recherche Avancées en Physique, Atomistilor 407, Magurele 077125, Romania³School of Science and Engineering, Reykjavik University, Menntavegur 1, IS-101 Reykjavik, Iceland⁴Science Institute, University of Iceland, Dunhaga 3, IS-107 Reykjavik, Iceland

(Received 19 June 2019; revised manuscript received 26 August 2019; published 12 September 2019)

We study the electronic transport through a pair of distant nanosystems (S_a and S_b) embedded in a single-mode cavity. Each system is connected to source and drain particle reservoirs and the electron-photon coupling is described by the Tavis-Cummings model. The generalized master equation approach provides the reduced density operator of the double system in the dressed-states basis. It is shown that the photon-mediated coupling between the two subsystems leaves a signature on their transient and steady-state currents. In particular, a suitable bias applied on subsystem S_b induces a photon-assisted current in the other subsystem S_a which is otherwise in the Coulomb blockade. We also predict that a transient current passing through one subsystem triggers a charge transfer between the optically active levels of the second subsystem even if the latter is not connected to the leads. As a result of backaction, the transient current through the open system develops Rabi oscillations (ROs) whose period depends on the initial state of the closed system.

DOI: [10.1103/PhysRevB.100.125416](https://doi.org/10.1103/PhysRevB.100.125416)**I. INTRODUCTION**

Promising applications of cavity quantum electrodynamics (QED) to spintronics are essentially rooted in the entangled dynamics of hybrid light-matter nanosystems. The presence of long-range electromagnetic coupling between distant quantum systems (ideally viewed as two qubits) has already been confirmed in self-assembled double quantum dots [1,2] and color centers embedded in photonic-crystal cavities [3]. In the field of circuit-QED Fink *et al.* [4] reported that the optical transmission spectrum of a superconducting qubits array embedded in a microwave resonator can be explained by relying on a Tavis-Cummings-Dicke Hamiltonian [5–7].

The Tavis-Cummings (TC) model provides the luminescence spectra and lasing properties of N two-level systems (TLS) interacting with a quantized radiation field [8]. Also, it allows one to investigate the N -photon Rabi splitting for two emitters having comparable coupling strengths [9]. As these calculations are meant to describe the outcome of optical measurements, the charge of each two-level subsystem is assumed to be conserved.

More recently, experimental setups were extended to cavity-coupled double quantum emitters connected to source/drain particle reservoirs as key components of cavity-QED optoelectronics [10,11]. Deng *et al.* [12] measured non-vanishing steady-state current correlations associated to a pair of distant graphene double QDs interacting with a microwave nanoresonator. The reflection amplitude of the latter displays a dip structure that was well fitted by the TC model and therefore proved the existence of nonlocal interaction through the microwave signal. In another work the detection of electron-phonon interactions relied on transport measurements for a

double-quantum dot defined in a suspended cavity-coupled InAs nanowire [13].

Let us recall here that electrostatically coupled quantum wires and parallel quantum dots (QDs) display Coulomb drag and charge sensing effects at nanoscale which were experimentally observed [14–16] and extensively studied from the theoretical point of view [17–20]. Of course, this capacitive coupling becomes ineffective as the distance between the two systems increases. It would also seem that in the absence of optical or microwave probe signals the Tavis-Cummings coupling cannot be turned on.

We hereby theoretically show that the photon exchange between distant mesoscopic conductors embedded in a microcavity can be activated by electronic transport. Let us consider two parallel nanowires, each one connected to a pair of source and drain particle reservoirs and embedded in a microcavity (see the sketch in Fig. 1). The subsystems S_a and S_b accommodate electrons with both spin orientations and could be also quantum dots or carbon nanotubes. The electron tunneling and the mutual Coulomb interaction between S_a and S_b are negligible.

Clearly, electrons tunneling from a source reservoir may relax before tunneling out to the drain reservoir, while the emitted photons interact with both subsystems. Then, in analogy with classical electrodynamics, one can look for antenna-like coupling in which the current established in one system generates an electromagnetic field (i.e., photons) which changes the quantum state of the other system. We confirm this idea by calculating the transient and steady-state currents of the double-emitter cavity system for two transport settings (see Sec. III).

On the theoretical side there are few works on transport through multiple quantum emitters. Schachenmayer *et al.* [21,22] emphasized that the presence of the cavity enhances the current through 1D chains embedded in a single-mode

*Corresponding author: valim@infim.ro

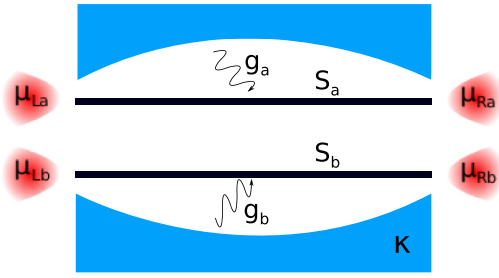


FIG. 1. Schematic view of two 1D nanowires S_a and S_b embedded in a single-mode cavity and individually coupled to source and drain leads. μ_{is} is the chemical potential of the lead i ($i = L, R$) attached to subsystem s ($s = a, b$) and g_s is the strength of the electron-photon interaction. The cavity losses are described by the parameter κ . The electron tunneling and the mutual Coulomb interaction between S_a and S_b are negligible.

cavity. Long distance coupling of resonant exchange qubits in the presence of the capacitive coupling to a transmission line has been studied by Russ and Burkhardt [23]. However, to the best of our knowledge, time-dependent transport calculations for distant parallel quantum emitters coupled by photons are not yet available.

The paper is organized as follows. The many-body Tavis-Cummings model, the structure of its dressed states, and the non-Markovian transport formalism are presented in Sec. II. The numerical results are discussed in Sec. III. Conclusions are left to Sec. IV.

II. FORMALISM

A. The Tavis-Cummings Hamiltonian of the double system

We shall now consider the Tavis-Cummings model for our many-body systems. The Hamiltonian H_s of each subsystem contains a noninteracting single-particle term and a two-particle Coulomb interaction within each subsystem (here $\sigma = \uparrow, \downarrow$ is the spin index and $s = a, b$):

$$H_s = \sum_{i,\sigma} \varepsilon_{is} c_{i\sigma}^\dagger c_{i\sigma} + \frac{1}{2} \sum_{\sigma,\sigma'} \sum_{i,j,k,l} v_{ijkl}^{(s)} c_{i\sigma}^\dagger c_{j\sigma'}^\dagger c_{l\sigma'} c_{k\sigma}. \quad (1)$$

The creation/annihilation operators $c_{i\sigma}^\dagger/c_{i\sigma}$ are associated to spin-dependent single-particle states $\psi_{i\sigma}^{(s)}$ of each subsystem. The eigenvalues ε_{is} are obtained by diagonalizing the single-particle Hamiltonian of the noninteracting double system. The wave functions $\psi_{i\sigma}^{(s)}$ inherit the size and geometry of the 1D nanowire. The matrix elements of the Coulomb interaction $v_{ijkl}^{(s)}$ are then calculated in terms of single-particle states $\psi_{i\sigma}^{(s)}$:

$$v_{ijkl}^{(s)} = \sum_{\alpha,\beta} \overline{\psi_{i\sigma}^{(s)}(\alpha)} \psi_{k\sigma}^{(s)}(\alpha) u(\alpha - \beta) \overline{\psi_{j\sigma'}^{(s)}(\beta)} \psi_{l\sigma'}^{(s)}(\beta), \quad (2)$$

where α, β are sites describing the subsystem S_s , $\overline{\psi_{i\sigma}^{(s)}}$ is the complex conjugate of the single-particle wave function and $u(\alpha - \beta)$ is the Coulomb potential. A small screening constant is added in the Coulomb kernel in order to avoid on-site singularities.

The interacting many-body states (MBSs) $|v\rangle$ and the associated energies E_v of the double system are defined as:

$$(H_a + H_b)|v\rangle = E_v|v\rangle. \quad (3)$$

Embedding this parallel structure in a single-mode cavity of frequency ω results in a hybrid system described by:

$$H_S = H_a + H_b + \hbar\omega\hat{a}^\dagger\hat{a} + \sum_{s=a,b} V_s := H_S^{(0)} + V_{\text{el-ph}}, \quad (4)$$

where V_s stands for the optical coupling between electrons in subsystem s and the cavity photons:

$$V_s = \sum_{i,j \in S_s} \sum_{\sigma} \hbar g_{ij}^{(s)} c_{i\sigma}^\dagger c_{j\sigma} (\hat{a}^\dagger + \hat{a}). \quad (5)$$

Note that the Hamiltonian H_S in Eq. (4) is more general than the Tavis-Cummings Hamiltonian encountered in quantum optics, as it acts on a many-body configuration space which includes the empty states of each subsystem and the spin degree of freedom. The optical selection rules are embodied in the constants $g_{ij}^{(s)}$, and in particular the spin σ is conserved. \hat{a}^\dagger denotes the photon creation operator and $\hbar\omega\hat{a}^\dagger\hat{a}|N\rangle = N\hbar\omega|N\rangle$ where $|N\rangle$ is the N -photon Fock state. The coupling constants are calculated as

$$g_{ij}^{(s)} = \frac{e}{m_0} \sqrt{\frac{\hbar}{2\epsilon\omega V}} \langle \psi_{i\sigma}^{(s)} | \mathbf{e} \cdot \mathbf{p} | \psi_{j\sigma}^{(s)} \rangle, \quad (6)$$

where \mathbf{p} is the momentum operator, \mathbf{e} is the polarization vector, ϵ is the dielectric constant, and V is the volume of the cavity. The matrix elements $g_{ij}^{(s)}$ in Eq. (6) are calculated numerically by discretizing the momentum operator and using its action on the site-dependent single-particle wave functions.

In the rotating wave approximation Eq. (5) counts only terms for which $\varepsilon_{js} < \varepsilon_{is}$ and V_s reduces to the well known Jaynes-Cummings (JC) optical coupling. We shall use the simplified notation $g_{12}^{(s)} = g_{21}^{(s)} := g_s$. Moreover, for identical subsystems one has $g_a = g_b = g_0$.

B. Energy spectrum and dressed states

In order to capture the main physics of the open hybrid system we shall adopt here a simple lattice model. A more accurate description of the cavity-coupled system requires a continuous model in spatial coordinates which was implemented in previous work [24–26].

Let $\varepsilon_{1s,2s}$ be the lowest spin-degenerate single-particle energies of subsystem s , ordered such that $\varepsilon_{1s} < \varepsilon_{2s}$ (i.e., $i = 1, 2$). In the absence of both Coulomb interaction and electron-photon coupling the many-body states of the double system are written in the occupation number basis associated to the single-particle states $\psi_{i\sigma}^{(s)}$. The occupation of such a state is specified by the spin σ_{is} . For example the state $|\uparrow_{1a}\downarrow_{2b}\rangle$ contains one electron on each subsystem, occupying the levels ε_{1a} and ε_{2b} and having the indicated spin orientations.

We start by diagonalizing the interacting many-body Hamiltonian $H_a + H_b$ of the double system on a reduced Fock space comprising all 256 noninteracting many-body configurations containing up to four electrons which are allowed to occupy the single-particle levels $\varepsilon_{1s,2s}$ of each subsystem S_s . For suitable values of the bias voltage applied on each nanowire the resulting interacting many-body states $|v\rangle$ provide a reliable basis for transport calculations. This choice reduces considerably the numerical cost of the time-dependent transport calculations but also captures the optical processes

involving only pairs of spin-degenerate single-particle lowest-energy states of each subsystem. The exact diagonalization method is not perturbative and therefore a suitable ‘small’ parameter does not present itself. Nonetheless, error estimates for interacting quantum dots have been calculated (see, e.g., the work of Kvaal [27], and the paper by Jeszenszki *et al.* on 1D quantum gases with contact interactions [28]). For the parameters selected in our calculations the relevant interacting many-body states are numerically stable when computed by diagonalizing the Hamiltonian on several truncated subspaces. Moreover, since the electron-photon coupling strength $g_0 \ll \omega$ the accuracy of the dressed states is even higher. The convergence of the exact diagonalization method for circuit quantum electrodynamics was thoroughly investigated in a previous publication [29].

Since there is no tunneling between S_a and S_b the electronic occupations $n_s^{(v)}$ of each subsystem s for a given MB configuration $|v\rangle$ are good quantum numbers:

$$n_s^{(v)} := \sum_{i \in S_s, \sigma} \langle v | c_{i\sigma}^\dagger c_{i\sigma} | v \rangle = \sum_i n_{is}^{(v)}. \quad (7)$$

Then the eigenstates $|v, N\rangle$ of the disjointed Hamiltonian $H_S^{(0)}$ [see Eq. (4)] can be organized in orthogonal subspaces labeled by particle and photon numbers $(n_a, n_b; N)$. For further use let us briefly describe these subspaces. The N -photon ‘empty’ states (i.e., without electrons) of the subspace $(0, 0; N)$ are denoted by $|0, N\rangle$. Next, one has four single-electron states $|\sigma_{is}, N\rangle$ for each subsystem, leading to the subspaces $(1, 0; N)$ and $(0, 1; N)$. The subspace $(1, 1; N)$ comprises 16 two-particle states which, when mixed by the electron-photon coupling generate the Tavis-Cummings dressed states (see below). Note that because the Coulomb interaction between the two subsystems is neglected the configurations belonging to this subspace can be simply written as $|\sigma_{ia}\sigma_{jb}, N\rangle$.

The internal Coulomb interaction effectively shows up in the subspaces $(2, 0; N)$ and $(0, 2; N)$. The degenerate two-particle ground states are $|G^{(s)}, N\rangle := |\uparrow_{1s} \downarrow_{1s}, N\rangle$, while the antiparallel and parallel triplet configurations are denoted by $|T_0^{(s)}, N\rangle$, $|T_1^{(s)}, N\rangle$. Finally, $|S^{(s)}, N\rangle$ stands for the singlet configurations. More complicated configurations can be constructed in a similar way.

Let $\mathcal{E}_{v,N}^{(0)} = E_v + N\hbar\omega$ be the energy of the ‘free’ state defined by $H_S^{(0)}|v, N\rangle = \mathcal{E}_{v,N}^{(0)}|v, N\rangle$. The fully interacting electron-photon Hamiltonian H_S is then diagonalized w.r.t. the basis $\{|v, N\rangle\}$ of the disjointed systems. Its eigenfunctions and eigenvalues are denoted by $|\varphi_p\rangle$ and \mathcal{E}_p such that

$$H_S|\varphi_p\rangle = \mathcal{E}_p|\varphi_p\rangle. \quad (8)$$

Here p is a set of relevant quantum numbers (see below). In the transport calculations the number of photons is truncated to N_{ph} , that is we allow at most $N_{\text{ph}} + 1$ Fock states to assist the transport. The electron-photon coupling mixes the ‘free’ states $|v, N\rangle$ but one finds that, besides the electronic occupations n_s on each subsystem, the excitation number $x = \sum_s n_{2s} + N$ is also conserved. Here n_{2s} is the occupation of the excited single-particle level ε_{2s} of S_s .

Up to spin-dependent quantum numbers, the fully interacting states are also organized in several subspaces described by the excitation number x and partial occupations n_a, n_b .

Obviously the ‘empty’ states are stable against the electron-photon coupling and one has $|\varphi_{N,0}\rangle := |0, N\rangle$. For the single-particle sector ($n_a + n_b = 1$) we get spin degenerate (optically active) dressed states $|\varphi_{N,\sigma_s}^\pm\rangle$ for each two-level system and some dark states:

$$|\varphi_{N,\sigma_s}^\pm\rangle = \frac{1}{\sqrt{2}}(|\sigma_{1s}, N+1\rangle \pm |\sigma_{2s}, N\rangle), \quad (9)$$

$$|\varphi_{0,\sigma_{1s}}\rangle = |\sigma_{1s}, 0\rangle, \quad |\varphi_{N_{\text{ph}},\sigma_{2s}}\rangle = |\sigma_{2s}, N_{\text{ph}}\rangle. \quad (10)$$

The excited state $|\varphi_{N_{\text{ph}},\sigma_{2s}}\rangle$ given by Eq. (10) cannot emit another photon because of truncation w.r.t. the Fock states. The energies of the dressed states $|\varphi_{N,\sigma_s}^\pm\rangle$ at resonance, that is when $\varepsilon_{2s} - \varepsilon_{1s} = \hbar\omega$ ($N \geq 0$), are:

$$\mathcal{E}_{N,\sigma_s}^\pm = \varepsilon_{2s} + N\hbar\omega \pm \frac{\hbar\Omega_N}{2}, \quad (11)$$

where $\Omega_N = 2g_0\sqrt{N+1}$ is the well known N -photon Rabi frequency of the two-level JC model. The electron-photon interaction also affects the two-particle sector ($n_a + n_b = 2$, $n_a = n_b = 1$). Let us introduce first the ground (G), doubly-excited (X), triplet (T), and singlet (S) spin-dependent Dicke states:

$$|G_{\sigma\sigma'}, N\rangle = |\sigma_{1a}\sigma'_{1b}, N\rangle, \quad (12)$$

$$|X_{\sigma\sigma'}, N\rangle = |\sigma_{2a}\sigma'_{2b}, N\rangle, \quad (13)$$

$$|T_{\sigma\sigma'}, N\rangle = \frac{1}{\sqrt{2}}(|\sigma_{2a}\sigma'_{1b}, N\rangle + |\sigma_{1a}\sigma'_{2b}, N\rangle), \quad (14)$$

$$|S_{\sigma\sigma'}, N\rangle = \frac{1}{\sqrt{2}}(|\sigma_{2a}\sigma'_{1b}, N\rangle - |\sigma_{1a}\sigma'_{2b}, N\rangle). \quad (15)$$

For identical emitters it can be shown that at resonance the two-particle dressed states have the following structure (for the simplicity of writing we omitted the spin indices of the two-particle configurations):

$$\begin{aligned} |\varphi_{N,\sigma\sigma'}^{(1)}\rangle &= \sqrt{\frac{N}{2N-1}}|X, N-2\rangle - \sqrt{\frac{N-1}{2N-1}}|G, N\rangle, \\ |\varphi_{N,\sigma\sigma'}^{(2,3)}\rangle &= \sqrt{\frac{N}{4N-2}}|G, N\rangle \pm \frac{1}{\sqrt{2}}|T, N-1\rangle \\ &\quad + \sqrt{\frac{N-1}{4N-2}}|X, N-2\rangle, \\ |\varphi_{N,\sigma\sigma'}^{(4)}\rangle &= |S, N-1\rangle. \end{aligned} \quad (16)$$

The above expressions generalize the spinless case discussed by Quesada [9]. Note these expressions hold as long as the Coulomb interaction between the two subsystems is negligible. One infers that the states $|\varphi_{N,\sigma\sigma'}^{(\alpha)}\rangle$ with $\alpha = 2, 3, 4$ exist only for $N \geq 1$ while $|\varphi_{N,\sigma\sigma'}^{(1)}\rangle$ is not defined for $N = 1$ and $|\varphi_{0,\sigma\sigma'}^{(1)}\rangle = |G_{\sigma\sigma'}, 0\rangle$. For a nonvanishing excitation number N one gets a subspace of Tavis-Cummings dressed states $\{|\varphi_{N,\sigma\sigma'}^{(\alpha)}\rangle\}$. If the cavity mode is slightly detuned from resonance the eigenvalues $\mathcal{E}_{N,\sigma\sigma'}^{(\alpha)}$ are still fourfold degenerate w.r.t. the spin indices and the coefficients of the ‘free’ states can only be obtained by numerical diagonalization. The structure of the fully interacting states is however not affected (i.e., the electron-photon coupling mixes the same ‘free’ states).

As for the corresponding energies one finds that at resonance:

$$\mathcal{E}_{N,\sigma\sigma'}^{(1)} = \mathcal{E}_{N,\sigma\sigma'}^{(4)} = \varepsilon_{1a} + \varepsilon_{1b} + N\hbar\omega \quad (17)$$

$$\mathcal{E}_{N,\sigma\sigma'}^{(2,3)} = \varepsilon_{1a} + \varepsilon_{1b} \pm \hbar g_0 \sqrt{4N - 2} + N\hbar\omega. \quad (18)$$

From Eqs. (17) and (18) we infer that within the Tavis-Cummings N -excitation subspace the dynamics is controlled by two Rabi frequencies $\tilde{\Omega}_N = 2g_0\sqrt{4N - 2}$ and $\tilde{\Omega}_N/2$ associated to the two spectral gaps $\mathcal{E}_{N,\sigma\sigma'}^{(2)} - \mathcal{E}_{N,\sigma\sigma'}^{(3)}$ and $\mathcal{E}_{N,\sigma\sigma'}^{(1)} - \mathcal{E}_{N,\sigma\sigma'}^{(2)}$. In fact by integrating numerically the von Neumann equation of the closed hybrid system described by H_S [see Eq. (4)] one finds that the populations of the optically active ‘free states’ and the mean photon number oscillate with periods associated to the above frequencies.

C. Generalized master equation method

We set our transport problem in the partitioning approach [30] by assuming that at some time instants t_{L_s} and t_{R_s} the subsystem S_s is smoothly coupled to left (L) and right (R) particle reservoirs having chemical potentials μ_{L_s}, μ_{R_s} (see the sketch in Fig. 1). The reservoirs are modeled as semi-infinite tight-binding chains supplying electrons with both spin orientations. The Hamiltonian of the open system is written as

$$H(t) = H_S + H_L + H_T(t), \quad (19)$$

where H_L is associated to the four leads and H_T is the lead-sample tunneling term containing time-dependent smooth switching functions χ_l (here $l = L_a, R_a, L_b, R_b$):

$$H_L = \sum_l \sum_\sigma \int dk \varepsilon_{k\sigma l} c_{k\sigma l}^\dagger c_{k\sigma l} \quad (20)$$

$$H_T(t) = \sum_{s,l} \sum_{i \in S_s, \sigma} \int dk \chi^l(t) (T_{ki}^{(ls)} c_{k\sigma l}^\dagger c_{i\sigma} + \text{H.c.}), \quad (21)$$

where $c_{k\sigma l}^\dagger$ is the creation operator on lead and k is the electronic momentum. For simplicity we impose spin conservation in the tunneling region such that the coupling parameter $T_{ki}^{(ls)}$ is spin independent. In the present model we take into account the dependence of the tunneling coefficient on the single-particle wave functions [31], that is $T_{ki}^{(ls)} = V_{l,s} \phi_k^{l*}(0_l) \psi_{i\sigma}^{(s)}(n_l)$ where 0_l is the site of the lead l which couples to the contact site n_l of the corresponding subsystem. $V_{l,s}$ is a constant input parameter. The four-lead geometry shown in Fig. 1 corresponds to nonvanishing parameters $V_{L_a,s} := V_{L_s}$ and $V_{R_a,s} := V_{R_s}$. We tune V_{l_s} such that the values of the tunneling rates $\Gamma_{ki}^{(LS)} = |T_{ki}^{(LS)}|^2$ are around few μeV . The spectrum of the semi-infinite leads is $\varepsilon_{k\sigma l} = 2t_L \cos k$, where t_L denotes the common hopping energy on the leads.

Using the Nakajima-Zwanzig projection technique one obtains an equation for the reduced density operator (RDO) of the hybrid system $\rho(t) = \text{Tr}_L\{W\}$, where W is the full density operator of the coupled system and Tr_L is the trace over the

leads’ degrees of freedom:

$$\begin{aligned} \dot{\rho}(t) = & -\frac{i}{\hbar} [H_S, \rho(t)] \\ & - \frac{1}{\hbar^2} \text{Tr}_L \left\{ \left[H_T(t), \int_{t_0}^t ds U_{t-s} [H_T(s), \rho(s) \rho_L] U_{t-s}^\dagger \right] \right\} \\ & - \frac{\kappa}{2} (a^\dagger a \rho(t) + \rho(t) a^\dagger a - 2a \rho(t) a^\dagger). \end{aligned} \quad (22)$$

In Eq. (22) $U_t = e^{-it(H_S+H_L)/\hbar}$ is the unitary evolution of the disconnected systems and ρ_L is the equilibrium density operator of the leads. The third line defines a Lindblad-type operator which takes into account cavity losses.

Note that in this basis the unitary evolution U_t is easily handled as it becomes a diagonal matrix. The matrix form of GME leads us to consider transitions between pairs of states $\{\varphi_p, \varphi_{p'}\}$ [32]. As an example, the generalized transition matrix element:

$$A_{pp'}^{(l)}(k) = \sum_s \sum_{i \in S_s, \sigma} T_{ki}^{(ls)} \langle \varphi_p | c_{i\sigma}^\dagger | \varphi_{p'} \rangle f_l(\varepsilon_{k\sigma l}), \quad (23)$$

captures the tunneling processes of electrons from the l th lead to all single-particle levels i of the parallel structure. The tunneling selection rules can be obtained by considering the nonvanishing matrix elements of the creation operator w.r.t. the basis $\{\varphi_p\}$. In the steady-state regime one expects to recover the Born-Markov approximation such that the tunneling is controlled by Fermi-Dirac weights $f_l(\mathcal{E}_p - \mathcal{E}_{p'})$. This points out that the energy $\mathcal{E}_p - \mathcal{E}_{p'}$ required to add an extra electron to some initial configuration $|\varphi_{p'}\rangle$ of the parallel structure must be below the chemical potential of the l th lead in order to allow the tunneling process leading to the final state $|\varphi_p\rangle$.

As an example, the simplest transition between the single-particle ground state $|\varphi_{0,\sigma_{1s}}\rangle$ to the dark two-particle ground state $|G_s\rangle = |\uparrow_{1s} \downarrow_{1s}\rangle$ requires the energy $\mu_{G_s} = \mathcal{E}_{G_s} - \mathcal{E}_{0,\sigma_{1s}} = \varepsilon_{1s} + U$, where U is a few meV shift due to the internal Coulomb interaction. If $\mu_{L_s, R_s} < \mu_{G_s}$ this tunneling process is suppressed and the double occupancy of the subsystem s is excluded.

The GME is solved numerically as an integrodifferential system of coupled equations for the matrix elements of ρ w.r.t the basis of dressed states $\{|\varphi_p\rangle\}$. Once the RDO is calculated the mean value of the total charge operator $Q_S = \sum_{s,i,\sigma} c_{i\sigma}^\dagger c_{i\sigma}$ is calculated as $\langle Q_S(t) \rangle = \text{Tr}_{\mathcal{F}}\{Q_S \rho(t)\}$, the trace being performed on the Fock space \mathcal{F} made by the eigenstates $|\varphi_p\rangle$ of the hybrid system. The left and right transient currents J_{L_s}, J_{R_s} are identified from the continuity equation:

$$\frac{d}{dt} \langle Q_S \rangle = \text{Tr}_{\mathcal{F}}\{Q_S \dot{\rho}(t)\} = \sum_s (J_{L_s}(t) - J_{R_s}(t)). \quad (24)$$

By using the cyclicity of the trace and fact that Q_S commutes with the bosonic operators one easily finds that loss term in the GME does not contribute directly to the currents. Nonetheless, it affects the matrix elements of the RDO which are fully contained in the dissipative term due to the leads. The photon number is given by:

$$\mathcal{N}(t) = \text{Tr}_{\mathcal{F}}\{\rho(t) \hat{a}^\dagger \hat{a}\}. \quad (25)$$

The average charge occupation of the single-particle levels ε_{is} is given by $q_{is}(t) = e \sum_\sigma \text{Tr}_{\mathcal{F}}\{\rho(t) c_{i\sigma}^\dagger c_{i\sigma}\}$ (here e denotes

the electron charge). It is also useful to introduce the total populations of the Jaynes-Cummings ($n_a + n_b = 1$) and Tavis-Cummings ($n_a = n_b = 1$) N -photon manifolds:

$$P_{JC,N}^{\pm}(t) = \sum_{s,\sigma} \langle \varphi_{N,\sigma_s}^{\pm} | \rho(t) | \varphi_{N,\sigma_s}^{\pm} \rangle, \quad (26)$$

$$P_{TC,N}^{(\alpha)}(t) = \sum_{s,\sigma} \langle \varphi_{N,\sigma_s}^{(\alpha)} | \rho(t) | \varphi_{N,\sigma_s}^{(\alpha)} \rangle. \quad (27)$$

The total populations of JC and TC states are then easy to calculate (we omit the time dependence for the simplicity of writing):

$$P_{JC,N} = \sum_{\lambda=\pm} P_{JC,N}^{(\lambda)}, \quad P_{TC,N} = \sum_{\alpha} P_{TC,N}^{(\alpha)}. \quad (28)$$

In the present work we use a generalized master equation approach which provides the dynamics of the many-body configurations in the presence of sequential tunneling processes. Other methods allow the calculations of full counting statistics (FCS) for interacting systems [33,34]. In particular, in the presence of driving voltages the stochastic path-integral approach of Altland *et al.* [35,36] predicts that massive fluctuations will exceed the average values.

III. NUMERICAL RESULTS AND DISCUSSION

Our parallel structure comprises two identical 1D nanowires of 50 nm each, described as a lattice chain of $N_x = 250$ sites. The lowest two single-particle energies are $\varepsilon_{1s} = 41.25$ meV and $\varepsilon_{2s} = 41.95$ meV. The numerical calculations were performed by taking into account up to two photons in the cavity and the thermal energy $k_B T = 50$ mK. However, at the end of this section we provide and discuss results obtained when the number of Fock states included in the calculations increases. Moreover, we neglected the cavity losses as for $\kappa \ll g_0$ we obtained similar results. The hopping energy on the leads $t_L = 1$ meV.

The interplay of sequential tunneling and photon emission/absorption processes leads to a complicated dynamics of the hybrid system. However one expects that for weak coupling to the leads some features of the unitary dynamics $U_t = e^{-itH_s/\hbar}$ of the closed system could still be present in the transport properties. In particular, the time-dependent charge occupations on each subsystems will be shown to exhibit periodic JC or TC Rabi oscillations.

We set the chemical potentials of the source leads μ_{La} and μ_{Lb} above the single-particle levels ε_{is} but well below the energies of the interacting two-particle configurations of the type ($n_a = 2, n_b = 0$) or ($n_a = 0, n_b = 2$). Then the internal Coulomb interaction prevents the population of states with more than one electron on each system. These states can be safely disregarded in the time-dependent transport calculations and the GME is solved within a truncated subspace made of 25 electronic MBSs for the double system and the Fock states containing up to two photons. In this setup electrons tunnel through the system only via configurations with one electron and the relevant optical transitions only involve the lowest single-particle levels ε_{1s} and ε_{2s} .

A. Removal of the Coulomb blockade

The first transport setup we considered reveals the switching from the Jaynes-Cummings dynamics of a single subsystem to the Tavis-Cummings dynamics of the photon-coupled double system. The chemical potential μ_{Ra} is chosen such that the single-particle level ε_{2a} lies well within the bias window $\mu_{La} - \mu_{Ra}$ and the lowest one ε_{1a} is below μ_{Ra} [see the inset in Fig. 2(a)]. The fact that each subsystem accommodates only up to one electron is also suggested by indicating the energy of the ground two-particle states $2\varepsilon_{1s} + U$, where U denotes the upward shift due to the internal Coulomb interaction. The chemical potential μ_{Rb} is set such that both single-particle levels of S_b are within the bias window. We use equal couplings to the leads, $V_{Ls} = V_{Rs}$.

We calculated the current passing through the upper nanowire (S_a) while keeping the lower system S_b disconnected from leads. The initial state is $|00, 0\rangle$, that is each nanowire is empty and there are no photons in the cavity. In this case the only optically active states belong to the JC subspace $|\varphi_{N,\sigma_a}^{\pm}\rangle$ since $n_a = 1$ and $n_b = 0$. Next, we repeat the calculations for the same initial state except that now *both* systems are simultaneously coupled to the leads in order to populate two-electron Tavis-Cummings dressed states.

Figure 2(a) presents the transient currents corresponding to the JC and TC transport configurations. In the absence of the second subsystem the steady-state current vanishes due to the Coulomb blockade and the lowest level ε_{1a} is nearly filled. This can be seen in the average electronic occupation of the ground (q_{1a}) and excited (q_{2a}) single-particle energy levels in Fig. 2(b). The charge occupations display few Rabi oscillations on their way to the steady state. Similar oscillations of the transient current were reported for a continuous model [37]. Here we find that in the JC regime the oscillation period is $T_0 = 39$ ps, which corresponds to the Rabi frequency Ω_0 . The average photon number also vanishes [see Fig. 2(c)] because the steady-state configuration is an equal weight combination of ground states $|G_{\sigma\sigma'}, 0\rangle$ (not shown).

In Fig. 2(a) we also show the transient currents J_{La} and J_{Lb} in the absence of the electron-photon coupling (see the blue and red dashed lines). As expected, the current through the system S_a vanishes due to the Coulomb blockade and no Rabi oscillations are noticed. In contrast, since the bias window on S_b allows tunneling processes even in the steady-state and the photon exchange with S_a is no longer present, J_{Lb} reaches a slightly larger value in the stationary regime.

Note that for excitonic systems like self-assembled QDs the corresponding ground state is the fully occupied valence band which can only be populated via electron relaxation from the conduction band followed by photon emission. In our system *both* ‘conduction’ (ε_{2s}) and ‘valence’ (ε_{1s}) levels can be fed from the source contacts. The direct tunneling to the lower single-particle states considerably hampers photon emission so we can restrict our numerical calculations to a few Fock states only.

In the TC setting the above picture changes considerably. Figure 2(a) shows that the current J_{La} does not vanish anymore in the steady state, which means that the tunnelings from the excited level ε_{2a} to the right contact are now allowed. This removal of the Coulomb blockade on subsystem S_a proves the

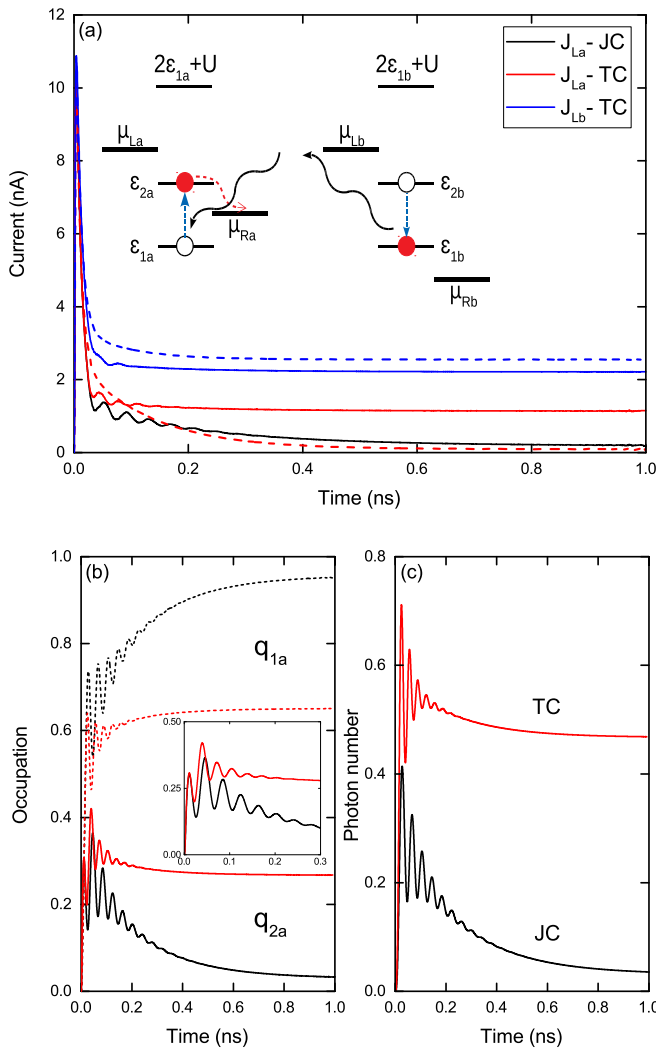


FIG. 2. (a) The current J_{La} (black solid line) vanishes in the steady state if the lower subsystem is disconnected. A current passing J_{Lb} on the lower subsystem S_b (blue solid line) removes the Coulomb blockade as suggested in the inset and a nonvanishing steady-state value of J_{La} is noticed (red solid line). The dashed lines represent the transient currents in the absence of the electron-photon coupling. Inset: A sketch of the low-energy levels of each subsystem and of the relevant processes in the removal of the Coulomb blockade: photon emission/absorption—black solid wavy line, electron relaxation/excitation—vertical dashed blue line, and tunneling to the leads—dashed red line. (b) The charge occupations on the optically active levels of S_a for the Jaynes-Cummings (dashed line) and Tavis-Cummings (solid line) transport configurations. Inset: q_{2a} in the transient regime. (c) The mean photon number for JC and TC regimes. Other parameters: $\mu_{La} = \mu_{Lb} = 45$ meV, $\mu_{Ra} = 41.5$ meV, $\mu_{Rb} = 35$ meV. The electron-photon coupling strength $g_0 = 53$ μ eV, $\kappa = 0$.

correlations due to the photon exchange between the two systems. The mechanism leading to the removal of the Coulomb blockade is also suggested in the inset of Fig. 2(a): (i) With two levels within its bias window, subsystem S_b generates photons even in the steady-state [see the corresponding mean photon number in Fig. 2(c)]; (ii) a photon emitted by S_b excites electrons from the lowest level of S_a to the higher level

which in turn tunnels to the right lead and contributes to the transport.

This scenario is confirmed by Fig. 2(b) from which one checks that the occupation q_{2a} is now around 0.25 while the lowest level is not fully occupied. We also notice that in the TC regime the Rabi oscillations have a different period [see the inset of Fig. 2(b)]. This is expected because the JC and TC subspaces have different Rabi frequencies for the associated dynamics. We shall discuss this fact in the next subsection.

The steady-state current J_{Lb} through the lower subsystem is larger than J_{La} due to the fact that both levels ϵ_{ib} are within the bias window. Let us note that the position of the two levels w.r.t. bias window is crucial for the removal of the Coulomb blockade. We have checked that by decreasing the bias window on S_b (i.e., for $\mu_{Rb} = 41.5$ meV) both systems are simultaneously blocked in the steady state as their lowest levels are fully charged and below the bias window.

B. All-electrical ‘reading’ of a closed system

The setup presented in the previous subsection captures a steady-state effect of the photonic coupling of the two electronic systems. To illustrate transient effects of the photon-mediated interaction between the two subsystems let us consider a transport setup in which the lower nanowire S_b is again disconnected from leads but can still be correlated to the upper wire. We assume that subsystem S_b is prepared in some initial state $|v_b\rangle$ before passing a current through the nearby subsystem S_a at instant $t_0 = 0$. If the two systems exchange photons (i.e., when $n_b \neq 0$ and the resonant condition holds both for S_a and S_b) the transport through the open system S_a should depend on the dynamics in the closed system S_b . The chemical potential of the leads attached to S_a are set such that both single-particle levels are within the bias window and photons are generated even in the steady-state regime.

In Fig. 3 we show the transient currents J_{Ra} for three initial configurations $|v_b\rangle$ of the closed system specified by the spin-dependent occupation numbers of the single-particle states in S_b , i.e., $|0\rangle$, $|\uparrow_{1b}\rangle$, and $|\uparrow_{2b}\rangle$. Although for simplicity we considered only a spin up electron occupying the subsystem S_b a mixture of both spin orientations could be initialized as well without changing the results. Each figure contains results for two values of the electron-photon coupling strength, $g_0 = 13.25$ μ eV and $g_0 = 26.5$ μ eV. Note that the Rabi period increases as g_0 decreases. Also, to avoid a fast damping of the Rabi oscillations we reduced the coupling to the leads.

One notices at once that the output transient current develops oscillations whose period depends on the initial state of subsystem S_b . In fact, the three periods in Fig. 3 are approximatively given by the Jaynes-Cummings and Tavis-Cummings Rabi frequencies (see Sec. II B) as follows: $T_0 = 2\pi/\Omega_0$, $T_1 = 4\pi/\tilde{\Omega}_1 = \sqrt{2}T_0$, and $T_2 = 4\pi/\tilde{\Omega}_2 = \sqrt{2/3}T_0$. This effect can be viewed as a backaction of the ‘measured’ subsystem S_b on the ‘driving’ subsystem S_a .

To explain this behavior we recall that the charge occupations q_{ia} (which contribute to the current through S_a) are optically correlated to the occupations of the closed system q_{ib} . Then we compared the Rabi oscillations of q_{ia} and q_{ib} to the time-dependent currents. When the closed system S_b

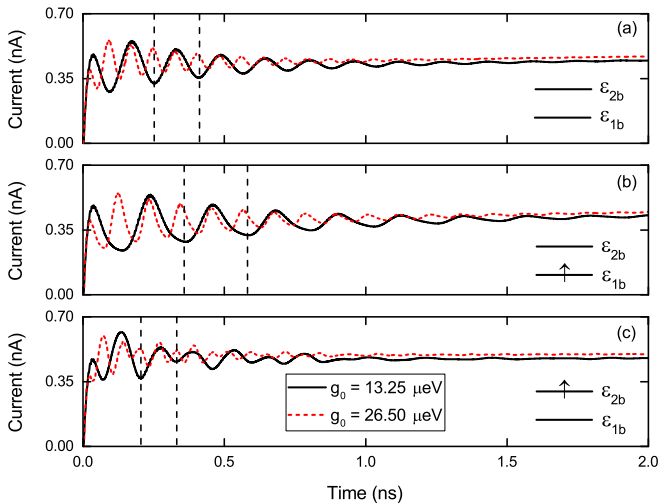


FIG. 3. The transient Rabi oscillations of the output current J_{Ra} corresponding to different initial states of the closed system. (a) $|0\rangle$, (b) $|\uparrow_{1b}\rangle$, and (c) $|\uparrow_{2b}\rangle$. The vertical dashed lines mark the Rabi oscillation period. The three initial configurations are also shown in the inset. Other parameters: $\mu_{La} = \mu_{Lb} = 45$ meV, $\mu_{Ra} = \mu_{Rb} = 35$ meV, $\kappa = 0$.

is not optically active (i.e., if it is either empty or set in the off-resonant regime w.r.t. the cavity mode) we have already seen that the occupations of the upper system S_a display transient Rabi oscillations with period T_0 (see Fig. 2 in Sec. III A).

If S_b is initialized in the state $|\uparrow_{1b}\rangle$ the photons emitted by S_a , where the electrons enter via sequential tunneling, activate the correlations between the two subsystems. These are confirmed by Figs. 4(a) and 4(b) which present out-of-phase

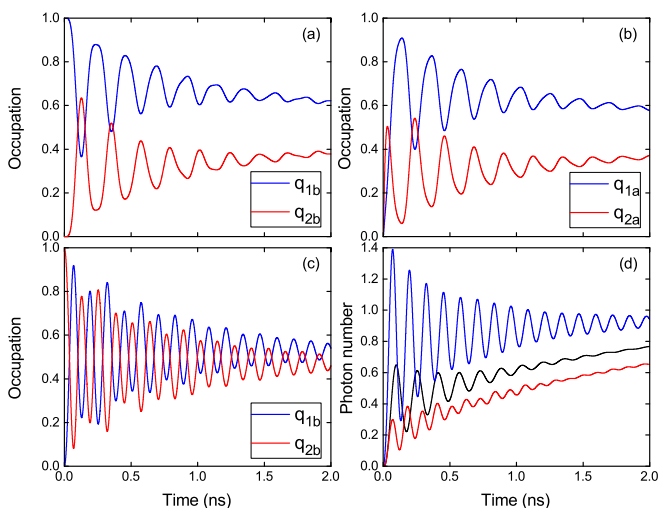


FIG. 4. The transient Rabi oscillations of the charge occupations q_{is} for different initial states of the closed system S_b . (a) q_{ib} for the initial state $|\uparrow_{1b}\rangle$. (b) q_{ia} for the initial state $|\uparrow_{1b}\rangle$. The out-of-phase oscillations are due to correlated processes of emission (absorption) of one photon by S_a and absorption (emission) by the electron on the lowest level in S_b . (c) q_{ib} for the initial state $|\uparrow_{2b}\rangle$. (d) The mean photon number \mathcal{N} for the three initial states: black— $|0\rangle$, red— $|\uparrow_{1b}\rangle$, blue— $|\uparrow_{2b}\rangle$. Other parameters: $\mu_{La} = 45$ meV, $\mu_{Ra} = 35$ meV, $g_0 = 13.25$ μ eV, $\kappa = 0$.

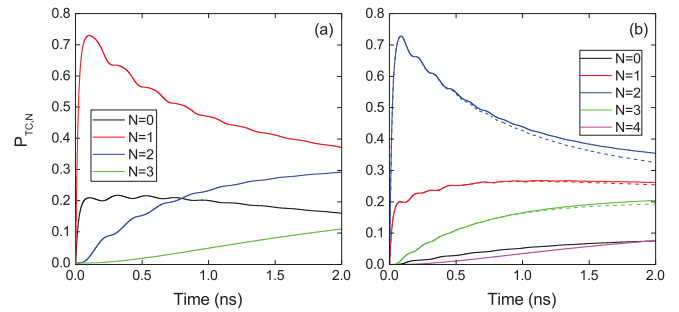


FIG. 5. The populations of the Tavis-Cummings dressed states with $N = 0, 1, 2, 3$ excitations for two initial states of the closed system S_b . (a) $|\uparrow_{1b}\rangle$, (b) $|\uparrow_{2b}\rangle$. In Fig. 5(b) we add (see the dashed lines for $N = 1, 2, 3$ and the solid line for $N = 4$) the populations obtained by suitably increasing the number of photonic Fock states taken into account in the numerical simulations. The parameters are the same as in Fig. 4.

oscillations of the occupations q_{ia} and q_{ib} . The oscillations in the charge occupations coincide with the ones in the output current from S_a . Finally, if subsystem S_b is prepared in the excited state $|\uparrow_{2b}\rangle$ the charge occupations follow the dynamics of the $N = 2$ TC subspace so the oscillation period of q_{ib} [see Fig. 4(c)] roughly decreases by a factor of $\sqrt{3}$ when compared to the $N = 1$ case. As expected, the charge oscillations of S_a are quickly dumped by the tunneling processes, while the oscillations in q_{ib} are clearly visible even at longer times.

The mean photon number is also shown in Fig. 4(d) for the three initial states of the closed system. The oscillation periods corresponding to the $N = 1$ TC subspace is $T_0/\sqrt{2}$, half the period of the charge occupations. On the other hand for $N = 2$ the mean photon number oscillates with the same period as q_{ib} . The different periods for q_{is} and \mathcal{N} is essentially due to the fact that the $N = 1$ manifold contains only three dressed states [see Eq. (16)]. In this case the unitary dynamics of the closed system in the ‘free’ basis shows that the population of the ground-state configurations $G_{\sigma\sigma',1}$ (which gives the only contribution to the mean photon number) follows the dynamics associated to the larger gap $\mathcal{E}_{\sigma\sigma'}^{(2)} - \mathcal{E}_{\sigma\sigma'}^{(3)}$. In contrast, the charge occupations obey a slower dynamics given by the smaller gap $\mathcal{E}_{\sigma\sigma'}^{(3)} - \mathcal{E}_{\sigma\sigma'}^{(1)}$, such that the oscillation period is twice the one of the photon number.

Since each oscillation period of J_{Ra} is associated to one initial state of S_b , the analysis of the transient current provides an all-electrical probing of the closed subsystem. Let us note that the steady-state values of the currents shown in Figs. 3(a)–3(c) do not offer any hint on the initial state of S_b or on the N -photon subspaces involved in transport.

A valuable insight on the system dynamics is provided by the time-dependent populations $P_{TC,N}$ associated to N -excitation Tavis-Cummings dressed states [see Eq. (28)]. If we switch the coupling to the leads with S_b in its single-particle ground state the transient regime [see Fig. 5(a)] is mostly described by single-excitation dressed states whose total population peaks up to 0.73 at short times and then slowly decreases towards the steady-state value. Higher excited states with $N = 2$ slowly emerge in the system dynamics as the generation of more than one photon becomes possible. One also notices that the total population of the

spin-degenerate ground states $|G_{\sigma\sigma'}, 0\rangle$ saturates quite fast at 0.2 and the contribution of the $N = 3$ configurations is negligible. One can therefore argue that the Rabi oscillation period of the transient current must correspond to the TC frequency $\tilde{\Omega}_1$.

If S_b is initially in the state $|\uparrow_{2b}\rangle$ the two-excitation configurations dominate the transient regime [see Fig. 5(b)], which again support the finding of the Rabi oscillation period given by $\tilde{\Omega}_2$. The single-excitation states, although not negligible, leave no clear fingerprint on the charge dynamics. The total population associated to the dressed states in the Jaynes-Cummings sector does not exceed 0.06 and therefore were not shown.

From Figs. 5(a) and 5(b) we also notice that the double-emitter system is described by a mixture of Tavis-Cummings dressed states living in subspaces with different excitation numbers N . This feature is never encountered in the absence of the leads, because the electron-photon interaction is block-diagonal w.r.t. the excitation number N . We find out that the coexistence of states with different excitation number is due to the interplay of the photon emission and tunneling in and out processes. Let us consider two possible ‘paths’ leading to a current in the upper system S_a . For simplicity we discuss elementary tunneling and optical processes involving the free states (we selected for simplicity a single spin orientation σ but more complicated combinations are also possible):

$$A : |\sigma_{2a}\sigma_{1b}, 0\rangle \rightarrow |\sigma_{1a}\sigma_{1b}, 1\rangle \rightarrow |\sigma_{1b}, 1\rangle \rightarrow |\sigma_{2a}\sigma_{1b}, 1\rangle,$$

$$B : |\sigma_{2a}\sigma_{2b}, 0\rangle \rightarrow |\sigma_{2a}\sigma_{1b}, 1\rangle \rightarrow |\sigma_{1b}, 1\rangle \rightarrow |\sigma_{1a}\sigma_{1b}, 1\rangle.$$

On path A an electron tunnels first on the upper level of subsystem S_a while S_b is on its ground state such that the hybrid system is in the state $|\sigma_{2a}\sigma_{1b}, 0\rangle$. Then a photon is emitted by S_a via electron relaxation on ε_{1a} . Next, the same electron tunnels to the right lead and the open system is charged by another electron which now occupies again the upper level ε_{2a} . By inspecting Eqs. (12)–(15) we notice that the states $|\sigma_{2a}\sigma_{1b}, 0\rangle$ and $|\sigma_{1a}\sigma_{1b}, 1\rangle$ are the building block of the $N = 1$ dressed states $|\varphi_{1,\sigma\sigma}^{(\alpha)}\rangle$ while the ‘final’ state $|\sigma_{2a}\sigma_{1b}, 1\rangle$ contributes to $N = 2$ states $|\varphi_{2,\sigma\sigma}^{(\alpha)}\rangle$. Clearly, the path A is more likely when S_b is set to the ground state $|\uparrow_{1b}\rangle$.

In turn, the 2nd path B is more likely when the closed subsystem S_b is in the excited state $|\uparrow_{2b}\rangle$. In this case a tunneling process on the excited level of S_a is followed by a photon emission in the closed subsystem S_b . Then as before a double tunneling involving both leads brings the system to $|\sigma_{1a}\sigma_{1b}, 1\rangle$.

In Fig. 5(b) we also show the populations of the Tavis-Cummings configurations calculated with a larger number of Fock states (i.e., the number of Fock states taken into account when solving the GME increases to $N_{\text{ph}} = 5$). One notices that new TC configurations with $N = 4$ excitations are slowly and rather poorly populated while the configurations with $N = 1, 2, 3$ decrease slightly [see the dashed lines in Fig. 5(b)]. The populations $P_{TC,N=5}$ and $P_{TC,N=6}$ turn out to be very small and were not shown. Note also that in the time range where one can read the initial state of the closed subsystem S_b from the Rabi oscillations of the transient current (i.e., for $t < 1$ ns) the addition of more photonic states does not lead to a noticeable change of $P_{TC,N}$ for $N = 0, 3$.

The correspondence between the transient ROs and the initial state of the closed system was recovered for other values of the electron-photon coupling strength g_0 ; this is expected as the ratio between the period of the ROs does not depend on g_0 . We also find that at fixed value of g_0 the number of clear ROs decreases at stronger coupling to the leads when the tunneling time becomes smaller than the Rabi periods. As for the effects of cavity losses, the above results are expected to hold as long as κ is much smaller than the electron-photon coupling strength. In particular, the period of the transient Rabi oscillations does not depend on κ .

Let us comment a bit more on the Coulomb interaction effects. If the chemical potentials μ_{L_S} are pushed upwards more complicated transitions between many-body configurations come into play. For example, the excited triplet or singlet states can relax to the two-particle ground state by photon emission at suitable frequency of the cavity. Then one expects corresponding Rabi oscillations in the transient currents and similar results. On the other hand, by adjusting the frequency to these new transitions one detunes the previous transitions between the single-particle levels. We also stress that in our calculations the initial state of the hybrid system corresponds to the vacuum field so the mechanism behind the revival of the population inversion is not activated. Moreover, here we are dealing with an open system and even if the initial photon configuration would be a superposition of different Fock states, the dissipation due to the sequential electron tunneling prevents the revival phenomenon.

In a recent experiment [38] the photons emitted by a voltage-biased double QD embedded in a microcavity are used to ‘read’ the charge state of a second unbiased double QD placed at the other side of the cavity. The ‘reading’ operation is performed by measuring the optical output power or the emission of the biased dot. In this context, our theoretical calculations predict the possible *electrical* readout of a ‘target’ subsystem by the transient current of the ‘probe’ subsystem.

IV. CONCLUSIONS

The transient and steady-state transport properties of parallel quantum conductors embedded in a photon cavity have been calculated from the generalized master equation. The system is described by a Tavis-Cummings model suitably extended for interacting and open systems. We propose two settings which exhibit clear effects of the coupling between the two conductors via cavity photons. A steady-state effect consists of the removal of a Coulomb blockade from one subsystem when a current passes through the second subsystem. This coincides with the switching between the Jaynes-Cummings dynamics of a single subsystem to the cavity-mediated Tavis-Cummings dynamics of the double system.

In a second setup we show that the photon-induced correlations provides information on the initial state of a closed subsystem by looking at the transient current which passes through a neighbor open subsystem. More precisely, the period of the Rabi oscillations of the ‘probing’ current depends of the initial state of the ‘probed’ system. Note that the ‘reading’ of the closed system via photon-mediated interactions

is far from being similar to the charge sensing based on mutual Coulomb interaction. The backaction effect reported here requires that the levels of the closed system are optically active, their gap roughly matching the frequency of the cavity mode. The interplay of photon emission/absorption processes and in/out sequential tunneling allows the simultaneous population of dressed states with different excitation number.

ACKNOWLEDGMENTS

The authors acknowledge financial support from CNCS - UEFISCDI Grant No. PN-III-P4-ID-PCE-2016-0221, from the Romanian Core Program PN19-03 (Contract No. 21 N/08.02.2019) and from Reykjavik University, Grant No. 815051. This work was also supported by the Research Fund of the University of Iceland, and the Icelandic Research Fund, Grant No. 163082-051.

-
- [1] A. Laucht, J. M. Villas-Bôas, S. Stobbe, N. Hauke, F. Hofbauer, G. Böhm, P. Lodahl, M.-C. Amann, M. Kaniber, and J. J. Finley, *Phys. Rev. B* **82**, 075305 (2010).
- [2] E. Gallardo, L. J. Martínez, A. K. Nowak, D. Sarkar, H. P. van der Meulen, J. M. Calleja, C. Tejedor, I. Prieto, D. Granados, A. G. Taboada, J. M. García, and P. A. Postigo, *Phys. Rev. B* **81**, 193301 (2010).
- [3] R. E. Evans, M. K. Bhaskar, D. D. Sukachev, C. T. Nguyen, A. Sipahigil, M. J. Burek, B. Machielse, G. H. Zhang, A. S. Zibrov, E. Bielejec, H. Park, M. Lončar, and M. D. Lukin, *Science* **362**, 662 (2018).
- [4] J. M. Fink, R. Bianchetti, M. Baur, M. Göppl, L. Steffen, S. Filipp, P. J. Leek, A. Blais, and A. Wallraff, *Phys. Rev. Lett.* **103**, 083601 (2009).
- [5] M. Tavis and F. W. Cummings, *Phys. Rev.* **170**, 379 (1968).
- [6] R. H. Dicke, *Phys. Rev.* **93**, 99 (1954).
- [7] B. M. Garraway, *Philos. Trans. R. Soc. London A* **369**, 1137 (2011).
- [8] F. P. Laussy, A. Laucht, E. del Valle, J. J. Finley, and J. M. Villas-Bôas, *Phys. Rev. B* **84**, 195313 (2011).
- [9] N. Quesada, *Phys. Rev. A* **86**, 013836 (2012).
- [10] M. Kulkarni, O. Cotlet, and H. E. Türeci, *Phys. Rev. B* **90**, 125402 (2014).
- [11] A. Cottet, M. C. Dartiaillh, M. M. Desjardins, T. Cubaynes, L. C. Contamin, M. Delbecq, J. J. Viennot, L. E. Bruhat, B. Douçot, and T. Kontos, *J. Phys.: Condens. Matter* **29**, 433002 (2017).
- [12] G.-W. Deng, D. Wei, S.-X. Li, J. R. Johansson, W.-C. Kong, H.-O. Li, G. Cao, M. Xiao, G.-C. Guo, F. Nori, H.-W. Jiang, and G.-P. Guo, *Nano Lett.* **15**, 6620 (2015).
- [13] T. R. Hartke, Y.-Y. Liu, M. J. Gullans, and J. R. Petta, *Phys. Rev. Lett.* **120**, 097701 (2018).
- [14] D. Laroche, G. Gervais, M. P. Lilly, and J. L. Reno, *Science* **343**, 631 (2014).
- [15] G. Shinkai, T. Hayashi, T. Ota, K. Muraki, and T. Fujisawa, *Appl. Phys. Express* **2**, 081101 (2009).
- [16] D. Bischoff, M. Eich, O. Zilberberg, C. Rössler, T. Ihn, and K. Ensslin, *Nano Lett.* **15**, 6003 (2015).
- [17] R. Sánchez, R. López, D. Sánchez, and M. Büttiker, *Phys. Rev. Lett.* **104**, 076801 (2010).
- [18] K. Kaasbjerg and A.-P. Jauho, *Phys. Rev. Lett.* **116**, 196801 (2016).
- [19] V. Moldoveanu, A. Manolescu, and V. Gudmundsson, *Phys. Rev. B* **82**, 085311 (2010).
- [20] B. N. Narozhny and A. Levchenko, *Rev. Mod. Phys.* **88**, 025003 (2016).
- [21] J. Schachenmayer, C. Genes, E. Tignone, and G. Pupillo, *Phys. Rev. Lett.* **114**, 196403 (2015).
- [22] D. Hagenmüller, S. Schütz, J. Schachenmayer, C. Genes, and G. Pupillo, *Phys. Rev. B* **97**, 205303 (2018).
- [23] M. Russ and G. Burkard, *Phys. Rev. B* **92**, 205412 (2015).
- [24] V. Gudmundsson, O. Jonasson, C.-S. Tang, H.-S. Goan, and A. Manolescu, *Phys. Rev. B* **85**, 075306 (2012).
- [25] O. Jonasson, C.-S. Tang, H.-S. Goan, A. Manolescu, and V. Gudmundsson, *New J. Phys.* **14**, 013036 (2012).
- [26] V. Gudmundsson, O. Jonasson, T. Arnold, C.-S. Tang, H.-S. Goan, and A. Manolescu, *Fortschr. Phys.* **61**, 305 (2013).
- [27] S. Kvaal, *Phys. Rev. B* **80**, 045321 (2009).
- [28] P. Jeszenszki, H. Luo, A. Alavi, and J. Brand, *Phys. Rev. A* **98**, 053627 (2018).
- [29] O. Jonasson, C.-S. Tang, H.-S. Goan, A. Manolescu, and V. Gudmundsson, *Phys. Rev. E* **86**, 046701 (2012).
- [30] C. Caroli, R. Combescot, P. Nozieres, and D. Saint-James, *J. Phys. C: Solid State Phys.* **4**, 916 (1971).
- [31] V. Moldoveanu, A. Manolescu, and V. Gudmundsson, *New J. Phys.* **11**, 073019 (2009).
- [32] I. V. Dinu, V. Moldoveanu, and P. Gartner, *Phys. Rev. B* **97**, 195442 (2018).
- [33] J. Cerrillo, M. Buser, and T. Brandes, *Phys. Rev. B* **94**, 214308 (2016).
- [34] M. Ridley, V. N. Singh, E. Gull, and G. Cohen, *Phys. Rev. B* **97**, 115109 (2018).
- [35] A. Altland, A. De Martino, R. Egger, and B. Narozhny, *Phys. Rev. Lett.* **105**, 170601 (2010).
- [36] A. Altland, A. De Martino, R. Egger, and B. Narozhny, *Phys. Rev. B* **82**, 115323 (2010).
- [37] V. Gudmundsson, A. Sitek, P.-Y. Lin, N. R. Abdullah, C.-S. Tang, and A. Manolescu, *ACS Photonics* **2**, 930 (2015).
- [38] Y.-Y. Liu, J. Stehlik, X. Mi, T. R. Hartke, M. J. Gullans, and J. R. Petta, *Phys. Rev. Appl.* **9**, 014030 (2018).